



# Investigation on the Clogging Behavior and Additional Wall Cooling for the Axial-Injection Cold Spray Nozzle

Xudong Wang, Bo Zhang, Jinsheng Lv, and Shuo Yin

(Submitted July 31, 2014; in revised form February 2, 2015)

During the cold spray process, nozzle clogging always happens when spraying low-melting point materials, e.g., aluminum, significantly decreasing the working efficiency. In this paper, a comprehensive investigation was carried out to clarify the reason for inducing nozzle clogging and then to evaluate a home-made nozzle cooling device for preventing nozzle clogging. Computational fluid dynamics technique was employed as the main method with some necessary experiment validation. It is found that the particle dispersion and the high-temperature nozzle wall at the near-throat region are two dominant factors that cause nozzle clogging. The numerical results also reveal that the home-made cooling device can significantly reduce the nozzle wall temperature, which was validated by the experimental measurement. Besides, the aluminum coating build-up experiment further indicates that the additional cooling device can truly prevent the nozzle clogging.

**Keywords** aluminum, cold spray, computational fluid dynamics (CFD), nozzle clogging, nozzle cooling

## 1. Introduction

Cold spraying is a relatively new coating technique developed in the mid-1980s and has been rapidly developing during the past two decades. In this process, powder particles (typically  $<50\ \mu\text{m}$ ) are accelerated to a high velocity ranging from 300 to 1200 m/s by a supersonic gas flow and then impinging onto a substrate in solid state without significant fusion, undergoing intensive plastic deformation. The 'low temperature' of cold spray particles can minimize the adverse effect brought by molten or semi-molten state, providing a possibility to coat oxygen-sensitive materials (Ref 1, 2). It has been widely accepted that there exists a material-dependent critical velocity for

a given condition (e.g., specific particle size, temperature, and material properties), only above which bonding at the particle/substrate interface can take place and the cold spray coating can be formed on the substrate surface (Ref 3-7).

Although cold spray technique can be used to fabricate many kinds of metal materials, nozzle clogging always happens, especially when using low-melting point particles or preheated particles, significantly decreasing the working efficiency. In general, it is believed that high temperature of the nozzle wall is the main factor inducing the occurrence of clogging. When low-melting point or preheated particles flow through the nozzle, collision occasionally takes place with the high-temperature nozzle inner wall, inducing the bonding between particles and nozzle wall and finally resulting in the nozzle clogging. This phenomenon may become more serious when using the nozzle with radial injection. Although this view is widely accepted, no directly experimental or theoretical evidences have been given to prove it.

In this study, this hypothesis was positively proved through the computational fluid dynamics (CFD) technique. Besides, a home-made cooling device of which the digital photo is shown in Fig. 1 was developed in order to deal with the high-temperature nozzle wall during the spray process. In some previous studies, CFD technique was also used to predict the temperature distribution within the nozzle wall and substrate in cold spray (Ref 8-10). Therefore, in the current study, the capability of the home-made cooling system for controlling the nozzle wall temperature was also evaluated by CFD method and partly validated by experimental measurement. The mass of cold-sprayed aluminum coatings produced with and without nozzle cooling was also compared to further evaluate the capacity of this cooling system.

**Xudong Wang**, School of Energy and Power Engineering, Dalian University of Technology, Dalian 116024, Liaoning, China and Dalian Boiler and Pressure Vessel Inspection Institute, Dalian 116013, Liaoning, China; **Bo Zhang** and **Jinsheng Lv**, School of Energy and Power Engineering, Dalian University of Technology, Dalian 116024, Liaoning, China; **Shuo Yin**, School of Energy and Power Engineering, Dalian University of Technology, Dalian 116024, Liaoning, China and IRTES-LERMPS (Laboratoire d'Etudes et de Recherches sur les Matériaux, les Procédés et les Surfaces), Université de Technologie de Belfort-Montbéliard, Site de Sévenans, 90010 Belfort Cedex, France. Contact e-mail: s.yin1984@hotmail.com.

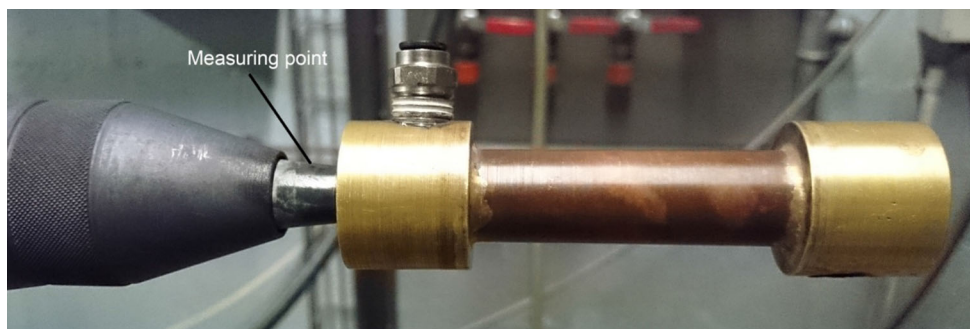


**Fig. 1** Digital photo of the cold spray nozzle and cooling device used in the experiment

**Table 1** Dimensions of the MOC nozzle

| Configuration                | Dimensions, mm |
|------------------------------|----------------|
| Throat diameter              | 2.7            |
| Inlet diameter (inner wall)  | 18.2           |
| Inlet diameter (outer wall)  | 26.7           |
| Outlet diameter (inner wall) | 6.4            |
| Outlet diameter (outer wall) | 11.2           |
| Cooling channel width        | 1.5            |
| Divergent length             | 120            |
| Convergent length            | 52.4           |

## 2. Numerical Methodology

### 2.1 Computational Domain and Boundary Conditions

Numerical simulations were performed using ANSYS-FLUENT 14.5 (Ref 11). The nozzle geometry was chosen according to the commercial MOC nozzle (CGT GmbH, Germany). The dimensions of the nozzle and cooling device are given in Table 1. The schematic of the computational domain is shown in Fig. 2. In order to save the computational time, the model was simplified as a two-dimensional axi-symmetric model. The computational domain was meshed into 240,200 quadrilateral cells in order to achieve a grid-independent solution. The grids at the nozzle throat region and impinging jet region were refined to accurately capture the rapid variation of flow properties due to the highly compressible character of the supersonic driving gas. The grid at the near-wall region was also refined to deal with the viscosity-affected region. The detailed boundary conditions of the computational model are listed in Table 2 in which the convective heat transfer coefficient ( $h$ ) is  $5 \text{ W/m}^2 \text{ K}$  and the free stream temperature is  $298 \text{ K}$ .

### 2.2 Modeling Details

Compressible air was chosen as the gas phase and controlled by ideal gas law. Liquid water was chosen as the coolant and treated as incompressible laminar flow. The thermal properties of air and water used in the simulation are listed in Table 3. The governing equations for a two-dimensional compressible and incompressible steady flows can be found elsewhere (Ref 12). Density-based implicit

**Table 2** Boundary conditions of the computational model

|                            | $P_0$                               | $v$                                 | $T_0$   |
|----------------------------|-------------------------------------|-------------------------------------|---|
| Gas inlet                  | Specified                           | $\frac{\partial v}{\partial n} = 0$ | Specified   |
| Coolant inlet              | 101,325                             | Specified                           | Specified   |
| Gas outlet, coolant outlet | 101,325                             | $\frac{\partial v}{\partial n} = 0$ | $\frac{\partial T}{\partial n} = 0$   |
| Axis                       | $\frac{\partial T}{\partial r} = 0$ | $\frac{\partial T}{\partial r} = 0$ | $\frac{\partial T}{\partial r} = 0$   |
| Outer wall                 | $\frac{\partial P}{\partial n} = 0$ | 0                                   | $-\kappa \cdot \frac{\partial T}{\partial n} = h \cdot (T - T_{\text{free}})$ |
| Inner wall                 | $\frac{\partial P}{\partial n} = 0$ | 0                                   | Coupled   |
| Substrate                  | $\frac{\partial P}{\partial n} = 0$ | 0                                   | $\frac{\partial T}{\partial n} = 0$   |

**Table 3** Properties of air and water used in the simulation

| Property               | Air                                  | Water                                |
|------------------------|--------------------------------------|--------------------------------------|
| Specific heat capacity | 1006.43 J/kg·K                       | 4182 J/kg·K                          |
| Thermal conductivity   | 0.0242 W/m·K                         | 0.6 W/m·K                            |
| Viscosity              | $1.789 \times 10^{-5} \text{ kg/ms}$ | $1.003 \times 10^{-3} \text{ kg/ms}$ |

solver was used to solve the steady flow inside and outside the nozzle due to its great capability to solve the strong compressible flow over pressure-based solver, such as high subsonic or supersonic problem. The RNG  $k$ - $\epsilon$  turbulence model was utilized to capture the turbulent flow features, and the enhanced wall function with refined mesh was chosen for the near-wall flow treatment.

Hard alloy and aluminum were chosen as the nozzle wall and particle materials, respectively. The thermal properties of the solid phase are listed in Table 4. The heat transfer process within the nozzle wall is governed by the two-dimensional energy equation for steady-state heat conduction (Ref 12). All the particles have the spherical shape. The trajectory of the particles was computed using discrete phase modeling (DPM) method which requires the discrete to be present at sufficiently low volume fraction. Particle-particle interactions and the effect of particles on the gas phase were neglected due to the low volume fraction of powder particles during the cold spray process (solid phase volume fraction  $< 10\%$ ). The high-mach-number drag law was applied to compute the particle drag force, which was always employed in previous studies (Ref 13-16). This drag

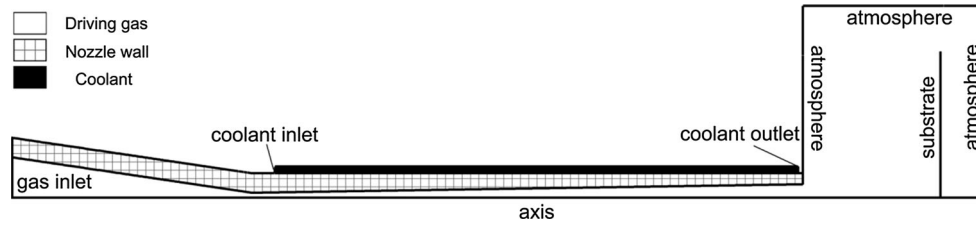


Fig. 2 Schematic of the computational domain of the CFD model used in the simulation

Table 4 Properties of hard alloy and aluminum used in the simulation

| Property             | Hard alloy               | Aluminum               |
|----------------------|--------------------------|------------------------|
| Density              | 14,800 kg/m <sup>3</sup> | 2719 kg/m <sup>3</sup> |
| Thermal conductivity | 80.0 W/m·K               | 202.4 W/m·K            |
| Heat capacity        | 210 J/kg·K               | 871 J/kg·K             |

law accounts for a particle Mach number greater than 0.4 at a particle Reynolds number greater than 20. The detailed description of this drag law can be found elsewhere (Ref 17). In order to take the turbulence-induced particle dispersion into consideration, the Stochastic-Tracking model available in ANSYS-FLUENT was used. In this approach, the discrete random walk (DRW) model is used to predict the fluctuating components of the total particle velocity and effects on its trajectory. When the path is computed for a sufficient number of times, a realistic prediction of the random effects by turbulence on particle dynamics can be achieved.

### 3. Experimental Validation

The nozzle outer wall temperature was measured by the thermocouple. The measuring point was selected at the position of 4 mm downstream from the nozzle throat. The thermocouple contacts to the nozzle outer wall surface directly and the data were recorded manually when the temperature becomes stable. Pure aluminum powders were selected as the feedstock to fabricate the cold-sprayed coating. The grit-blast copper plates were employed as the substrate. The main gas pressure and temperature were set as 2.5 MPa and 873 K, respectively. The substrate was located 30 mm away from the nozzle exit. A gun traverse speed of 50 mm/s was employed for the coating deposition. The mass of the coating produced with and without nozzle cooling was measured and compared to evaluate the cooling effect and the consequent nozzle clogging level.

## 4. Results and Discussion

### 4.1 Nozzle Clogging Behavior

In this section, the reason for inducing nozzle clogging is discussed. Figure 3 shows the trajectories of aluminum

particles inside the nozzle colored by particle velocity at the inlet pressure of 2.5 MPa and temperature of 873 K. It is seen that particles with different sizes disperse at the end of the convergent part due to the strong turbulent effect (Ref 18). Smaller particles show more significant dispersion than larger particles, almost occupying the entire divergent section. The collision between particles and nozzle inner wall can be clearly observed, particularly at the small zone before the throat section, which provides an essential condition for nozzle clogging. However, from Fig. 3, it is also noticed that the particle velocity prior to the impact at the near-throat section is not too high ( $< 300$  m/s) and the impact angle is quite small ( $< 30^\circ$ ). In this case, the normal particle impact velocity is lower than 150 m/s, which is below the critical velocity of aluminum. Coating is impossible to grow under this condition and nozzle clogging cannot occur. Therefore, there must be additional factors inducing nozzle clogging.

Previous work reported that the high-temperature region of the nozzle wall mainly locates at the convergent part and the following near-throat region where particle dispersion takes place (Ref 9). Similar result was also obtained in this study and given in Fig. 4 showing the temperature distribution within the nozzle wall at different working conditions. In cold spray, substrate preheating is found to facilitate the particle deposition and coating build-up process, significantly reducing the critical velocity (Ref 19-21). Here, the high-temperature nozzle wall plays the same role as the preheated substrate, helping to reduce the critical velocity of cold-sprayed particles on the nozzle wall and thus promoting the growth of blockage. Besides, particle temperature at the convergent part is also known to be relatively high due to the heating by the driving gas (Ref 13). Therefore, the impact between the particles and nozzle wall can be regarded as the preheated particle involved impact which also contributes to the particle deposition and the critical velocity reduction (Ref 22, 23). Hence, it is easy to conclude that the high-temperature nozzle wall and particle at the near-throat region is the above-mentioned additional reason for inducing nozzle clogging.

### 4.2 Evaluation of Nozzle Cooling for Preventing Nozzle Clogging

Knowing the reason for inducing nozzle clogging, one may attempt to find a solution way to avoid it. Particle velocity and temperature are really difficult to be controlled during the spray process, thus the most effective

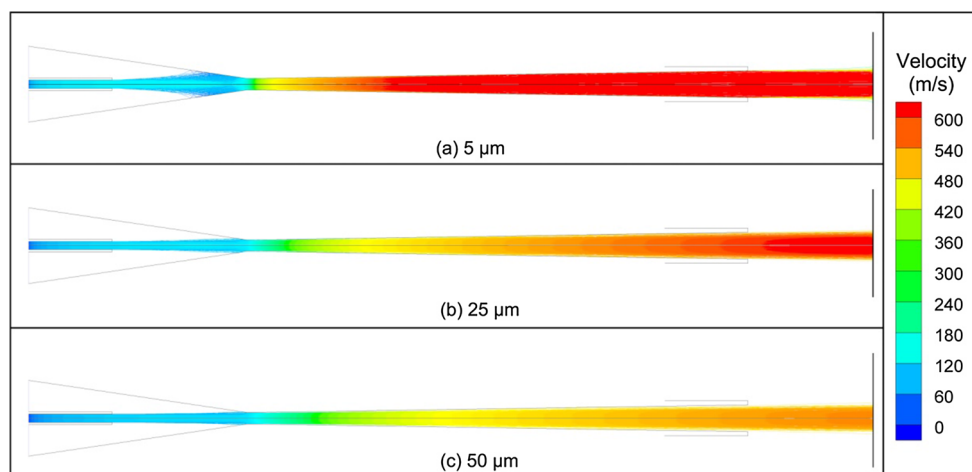


**Fig. 3** Trajectories of aluminum particles with different diameters inside the nozzle

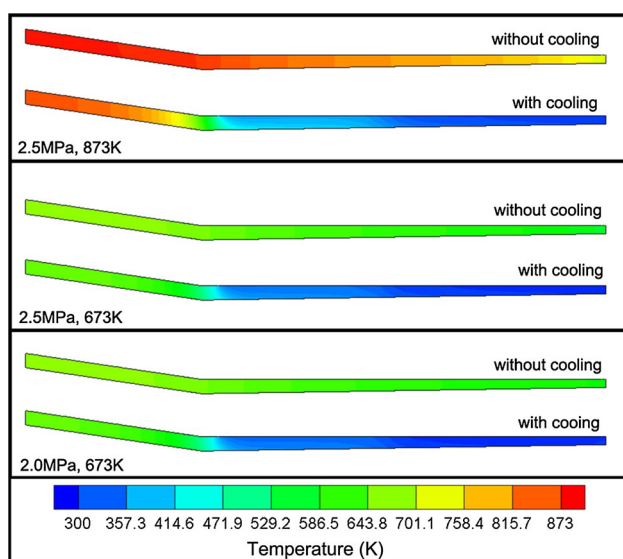


**Fig. 4** Temperature distribution within the nozzle at different working conditions with and without cooling

way may be to control the nozzle wall temperature. In this respect, a home-made cooling device was developed and installed at the divergent part to cool down the nozzle wall. Figure 4 shows the comparison of the temperature distribution within the nozzle wall with and without nozzle cooling. It is immediately seen that the nozzle wall temperature can be significantly decreased using additional cooling device, and the cooling effect at the divergent part is much better than that at the convergent part. This is because the additional coolant significantly increases the convective heat transfer between the nozzle wall and the surrounding environment. Table 5 gives the total surface heat transfer rate through the nozzle inner wall with and without nozzle cooling. Clearly, water as the coolant can take away more heat from the nozzle, leading to the temperature reduction of the nozzle wall. In order to

**Table 5** Total heat transfer rate through the nozzle inner wall

|                | Cooling, W | No-cooling, W |
|----------------|------------|---------------|
| 2.5 MPa, 873 K | 20.065     | 1624.891      |
| 2.5 MPa, 673 K | 12.943     | 1086.638      |
| 2.0 MPa, 873 K | 12.922     | 963.898       |

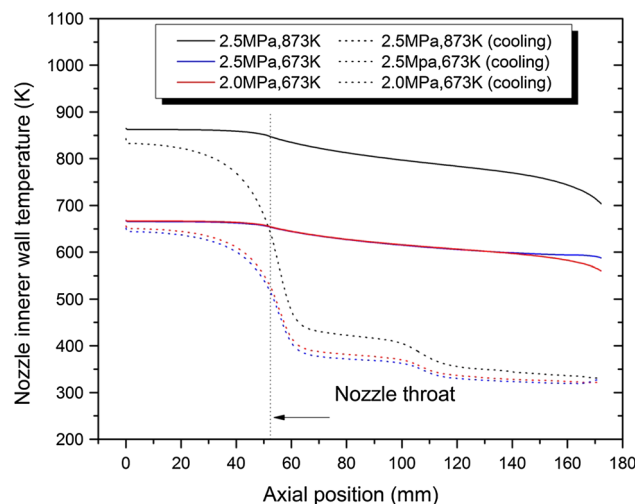
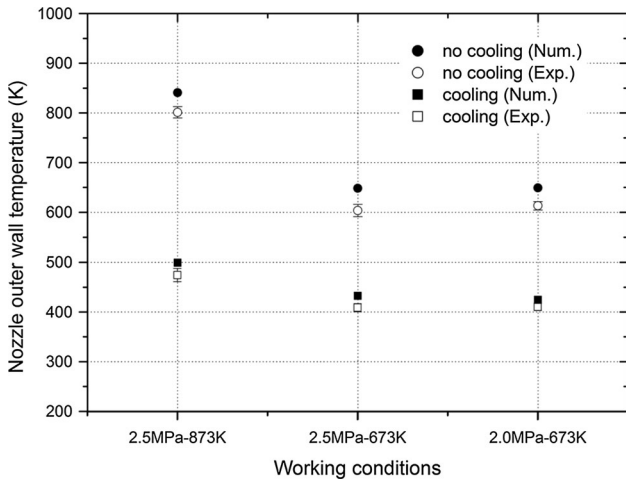


**Fig. 5** Nozzle inner wall temperature against the axial position at different working conditions with and without cooling

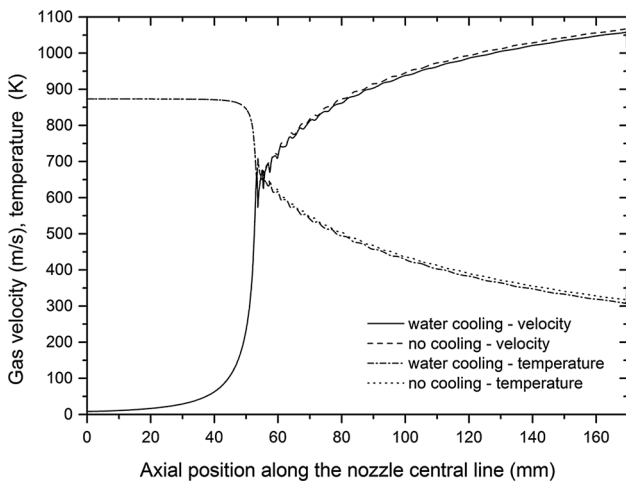
further analyze the temperature reduction on the nozzle inner wall, the inner wall surface temperature along the nozzle central line is given in Fig. 5. Obviously, cooling device can significantly reduce the nozzle inner wall temperature, especially at the throat and divergent part. It can be expected that the nozzle clogging can be improved under such conditions.

Figure 6 shows the comparison of the nozzle outer wall temperature between the simulation result and the ex-





**Fig. 6** Comparison of the simulation results to the experimental measurement



**Fig. 7** Gas velocity and temperature along the nozzle central line with and without cooling

perimental measurement. As can be seen, the predicted temperature compares fairly well with the experimental one, which positively proves the simulation result in this study. Besides, the mass of the cold-sprayed aluminum coatings produced with and without nozzle cooling was also measured. The one with nozzle cooling gives the coating mass of nearly four times higher than that without nozzle cooling because no clogging occurs inside the cooling nozzle. This fact further confirms that nozzle cooling helps to reduce the nozzle temperature and thus prevent the nozzle clogging.

Figure 7 provides the driving gas temperature and velocity along the nozzle central line under different cooling conditions. It is obvious that the driving gas temperature and velocity decrease when using cooling nozzle, but the reduction is quite limited, which is insufficient to pose any effects on the particle motion. This fact implies that nozzle cooling has no effects on the particle acceleration and the consequent coating build-up processes. In addition, for the

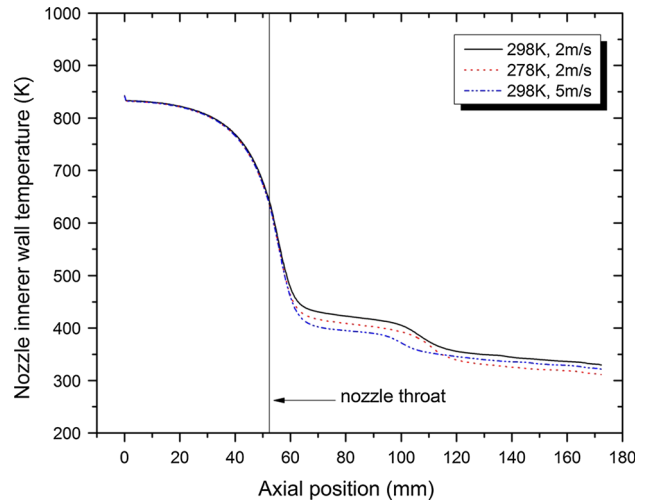


**Fig. 8** Nozzle inner wall temperature along the axial position at different cooling conditions

purpose to evaluate the effect of coolant conditions on the cooling effect, Fig. 8 shows the nozzle inner wall temperature along the nozzle central line at different cooling conditions. It is seen that increasing the water flow rate or decreasing the water temperature enhances the nozzle cooling, but such effect is quite slight. Therefore, considering the economics and conveniences, the room temperature piped water is sufficiently effective to cool down the cold spray nozzle.

## 5. Conclusions

In this study, the nozzle clogging behavior and nozzle cooling during cold spray process were systematically investigated by both numerical and experimental methods. Based on the obtained results, it is found that nozzle clogging was mainly induced by two essential factors which are particle dispersion and high-temperature nozzle wall at the near-throat region. The former allows the particles to impact on the nozzle inner wall and the latter promotes the growth of blockage. For solving this problem, a home-made cooling device was developed and equipped with the original cold spray nozzle to cool down the nozzle wall. The numerical results indicate that cooling system significantly decreases the nozzle wall temperature by enhancing the convective heat transfer, which is also validated by experimental data. Furthermore, the comparison of the mass of cold-sprayed aluminum coating produced with and without cooling system confirms that nozzle cooling truly prevents the nozzle clogging. Despite the fact that cooling system results in more heat loss of the driving gas, the gas temperature and velocity are not seriously affected, which means nozzle cooling has no effect on the gas and particle acceleration processes. Besides, increasing the water velocity or decreasing the water temperature can promote the cooling effect, but the room temperature piped water is found to be sufficiently effective to cool down the cold spray nozzle.



## Acknowledgments

The authors would like to acknowledge the support by Marie Curie FP7-IPACTS-268696 (EU).

## References

1. A.P. Alkhimov, V.F. Kosareve, and A.N. Papyrin, A Method of Cold Gas-Dynamic Spray Deposition, *Dokl. Akad. Nauk SSSR*, 1990, **315**(5), p 1062-1065
2. A. Papyrin, Cold Spray Technology, *Adv. Mater. Process.*, 2001, **159**(9), p 49-51
3. H. Assadi, Bonding Mechanism in Cold Gas Spraying, *Acta Mater.*, 2003, **51**(15), p 4379-4394
4. M. Grujcic, C.L. Zhao, W.S. DeRosset, and D. Helfrich, Adiabatic Shear Instability Based Mechanism for Particles/Substrate Bonding in the Cold-Gas Dynamic-Spray Process, *Mater. Des.*, 2004, **25**(8), p 681-688
5. T. Schmidt, F. Gärtner, H. Assadi, and H. Kreye, Development of a Generalized Parameter Window for Cold Spray Deposition, *Acta Mater.*, 2006, **54**(3), p 729-742
6. G. Bae, S. Kumar, S. Yoon, K. Kang, H. Na, H.-J. Kim, and C. Lee, Bonding Features and Associated Mechanisms in Kinetic Sprayed Titanium Coatings, *Acta Mater.*, 2009, **57**(19), p 5654-5666
7. H. Assadi, T. Schmidt, H. Richter, J.O. Kliemann, K. Binder, F. Gärtner, T. Klassen, and H. Kreye, On Parameter Selection in Cold Spraying, *J. Therm. Spray Technol.*, 2011, **20**(6), p 1161-1176
8. S. Yin, X.-F. Wang, W.-Y. Li, and X.-P. Guo, Examination on Substrate Preheating Process in Cold Gas Dynamic Spraying, *J. Therm. Spray Technol.*, 2011, **20**(4), p 852-859
9. W.-Y. Li, S. Yin, X. Guo, H. Liao, X.-F. Wang, and C. Coddet, An Investigation on Temperature Distribution Within the Substrate and Nozzle Wall in Cold Spraying by Numerical and Experimental Methods, *J. Therm. Spray Technol.*, 2011, **21**(1), p 41-48
10. S.H. Zahiri, T.D. Phan, S.H. Masood, and M. Jahedi, Development of Holistic Three-Dimensional Models for Cold Spray Supersonic Jet, *J. Therm. Spray Technol.*, 2014, **23**(6), p 919-933
11. ANSYS Fluent 14.5, User Guide, 2012
12. H.K. Versteeg and W. Malalasekera, *An Introduction to Computational Fluid Dynamics*, Pearson Education Limited, Harlow, 2007
13. S. Yin, M. Zhang, Z. Guo, H. Liao, and X. Wang, Numerical Investigations on the Effect of Total Pressure and Nozzle Divergent Length on the Flow Character and Particle Impact Velocity in Cold Spraying, *Surf. Coat. Technol.*, 2013, **232**, p 290-297
14. R. Lupoi and W. O'Neill, Powder Stream Characteristics in Cold Spray Nozzles, *Surf. Coat. Technol.*, 2011, **206**(6), p 1069-1076
15. T. Han, Z. Zhao, B.A. Gillispie, and J.R. Smith, Effects of Spray Conditions on Coating Formation by the Kinetic Spray Process, *J. Therm. Spray Technol.*, 2005, **14**(3), p 373-383
16. H. Tabbara, S. Gu, D.G. McCartney, T.S. Price, and P.H. Shipway, Study on Process Optimization of Cold Gas Spraying, *J. Therm. Spray Technol.*, 2010, **20**(3), p 608-620
17. R. Clift, J.R. Grace, and M.E. Weber, 'Bubbles, Drops, and Particles'. Technical Report. Academic Press, 1978
18. S. Yin, Q. Liu, H. Liao, and X. Wang, Effect of Injection Pressure on Particle Acceleration, Dispersion and Deposition in Cold Spray, *Comput. Mater. Sci.*, 2014, **90**, p 7-15
19. M. Fukumoto, H. Wada, K. Tanabe, M. Yamada, E. Yamaguchi, A. Niwa, M. Sugimoto, and M. Izawa, Effect of Substrate Temperature on Deposition Behavior of Copper Particles on Substrate Surfaces in the Cold Spray Process, *J. Therm. Spray Technol.*, 2007, **16**(5-6), p 643-650
20. P.C. King, G. Bae, S.H. Zahiri, M. Jahedi, and C. Lee, An Experimental and Finite Element Study of Cold Spray Copper Impact onto Two Aluminum Substrates, *J. Therm. Spray Technol.*, 2009, **19**(3), p 620-634
21. S. Yin, X.K. Suo, H.L. Liao, Z.W. Guo, and X.F. Wang, Effect of Preheated Substrate on the Deposition Mechanism of Cold Sprayed Copper Particles, *Proceedings of 6RIPT*, Limoge, 2013
22. S. Yin, X. Wang, X. Suo, H. Liao, Z. Guo, W. Li, and C. Coddet, Deposition Behavior of Thermally Softened Copper Particles in Cold Spraying, *Acta Mater.*, 2013, **61**(14), p 5105-5118
23. K. Kim, M. Watanabe, and S. Kuroda, Bonding Mechanisms of Thermally Softened Metallic Powder Particles and Substrates Impacted at High Velocity, *Surf. Coat. Technol.*, 2010, **204**(14), p 2175-2180